International Journal of Radiology and Diagnostic Imaging

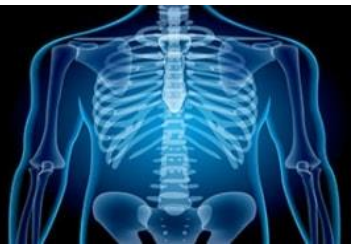

E-ISSN: 2664-4444
P-ISSN: 2664-4436
IJRDI 2019; 2(2): 96-105
Received: 17-05-2019
Accepted: 19-06-2019

Dr. Amit A Choure
Post Graduate Resident, Dr. D. Y. Patil Medical College, Hospital and Research Centre, Dr. D.Y. Patil Vidyapeeth, Pimpri, Pune, Maharashtra, India

Dr. Sanjay M Khaladkar
Professor, Dr. D. Y. Patil Medical College, Hospital and Research Centre, Dr. D.Y. Patil Vidyapeeth, Pimpri, Pune, Maharashtra, India

Dr. Suhani Jain
Post Graduate Resident, Dr. D. Y. Patil Medical College, Hospital and Research Centre, Dr. D.Y. Patil Vidyapeeth, Pimpri, Pune, Maharashtra, India

Corresponding Author:
Dr. Amit A Choure
Post Graduate Resident, Dr. D. Y. Patil Medical College, Hospital and Research Centre, Dr. D.Y. Patil Vidyapeeth, Pimpri, Pune, Maharashtra, India

Differentiation of benign and malignant cervical lymph nodes on MRI with special emphasis on DWI

Dr. Amit A Choure, Dr. Sanjay M Khaladkar and Dr. Suhani Jain

DOI: http://dx.doi.org/10.33545/26644436.2019.v2.i2b.46

Abstract
Aim and objectives: Evaluation of cervical lymph nodes with MRI, utility of DWI in differentiation of benign and malignant cervical lymph nodes.
Methods: Prospective study was carried out on 71 patients of cervical lymphadenopathy in Dr. D.Y. Patil Medical College, Hospital and Research Centre, Pimpri, Pune over a period of two years. Patients were evaluated with Siemens MAGNETOM Avanto 1.5 T MRI machine. Characteristics of cervical lymph nodes on T1WI, T2WI, STIR and Diffusion weighted images with ADC values were studied. Comparison was made with histopathological reports to study accuracy of MRI DWI in differentiating benign and malignant lymph nodes.
Results: Out of the total 71 cases, 41 cases were of benign lymph nodes and 30 cases were of malignant lymph nodes. Characteristics of lymph nodes were studied on MRI. Malignant lymph nodes showed diffusion restriction with corresponding low ADC values. Mean ADC value of benign lymph nodes was $1.1\times10^{-3}mm^2/s$ (±0.9 SD) and for malignant lymph nodes was $0.7\times10^{-3}mm^2/s$ (±0.2 SD).The suggested ADC cut off value in our study for differentiating benign from malignant lymph nodes was to be 0.93×10^{-3} mm^2/s.
Conclusion: Diffusion weighted imaging (DWI) is an important non-invasive diagnostic method for differentiation of benign and malignant cervical lymph nodes in case of head, neck cancers.

Keywords: Lymph nodes, malignant, cervical, diffusion weighted, apparent diffusion coefficient

Introduction
Location of cervical lymph nodes and their imaging characteristics are extremely important in differentiating between benign and malignant cervical lymph nodes [1].
Cervical lymph node enlargement can occur due to benign etiology like infections (Bacterial, Viral, granulomatous), malignant (Primary-lymphoma or metastatic) and miscellaneous (Eoisonophilic granulomas, Histiocytosis, Kikuchi's disease, Kimura's disease, Castlemen's disease) [2].
It also plays an important role in surgical treatment plan and determining the prognosis [3].
Morphological features like size of lymph nodes, shape, vascularity, extra capsular spread, calcifications, presence of necrosis are used for the diagnosis of malignancy. These parameters are not enough for differentiating the benign and malignant lymph nodes [4]. Diffusion weighted MRI (DW-MRI) is superior in detecting nodal metastasis [5]. Diffusion weighted image (DWI) is a non-invasive functional technique to study the molecular function and micro-structure of the tissue and lesion. Apparent diffusion coefficient and signal intensity in DWI and ADC maps are based on the analysis of water molecule motion. As the architectural structure of the tissue changes it will alter the ADC coefficient and signal intensity in DWI and ADC maps [6].
USG guided FNAC though fairly accurate is an invasive procedure and completely operator dependent with high incidence of false negative results [7].
Magnetic resonance with diffusion weighted imaging (DWI) is a non-invasive technique which could improve the diagnostic accuracy in differentiating between benign and malignant lymph nodes by measuring their ADC values; hence we have conducted this study. Comparison of MRI results with histopathology was done.

Materials and Methods
Prospective study was carried out on 71 patients of cervical lymphadenopathy in Dr. D.Y. Patil Medical College, Hospital and Research Centre, Pimpri,

Pune over a period of two years after clearance from Institutional Ethical Committee (IEC). Patients were evaluated with Siemens MAGNETOM Avanto 1.5 T MRI machine.

MR protocol

- T1W-FSE-axial and sagittal: TR: 400ms, TE: 20ms, slice thickness: 3 mm, Matrix: 320×320, NXA:2
- T2W-FSE-axial and coronal: TR: 4000ms, TE: 110ms, slice thickness: 5 mm, Matrix: 320×320, NXA:2
- STIR-axial and coronal: TR: 4500ms, TE: 40ms, TI: 160ms, slice thickness: 4.5mm, matrix: 256×256, NXA:2
- T1W-axial-fat sat: TR: 400ms, TE: 20ms, slice thickness: 3 mm, Matrix: 320×332, NXA:2

Acquisition of diffusion-weighted images using single shot echo planar imaging (EPI) sequence was achieved in the axial plane. Diffusion gradient encoding was done in the three planes (X, Y, Z) with three b values, b=0, b=500 and b=1,000 s/mm^2.

Imaging parameters for DWI were as follows: TR= 400-600ms, TE= 80ms, Matrix size=136×160, slice thickness = 3mm, NXA=2. The ADC map was calculated automatically using a standard software imager in the MR system.

In addition, contrast-enhanced MRI scan is provided in sagittal, coronal and axial planes for each patient in order to confirm the localization of malignant tissue as well as any cysts or necrosis. Informed consent and written consent was obtained from all the patients.

Patients of all age groups and both sexes detected to have cervical lymphadenopathy clinically and sono-graphically, whose size was more than 5mm were included. Completely necrotic lymph nodes, post radiation and post-operative lymph nodes, patient having history of cardiac pacemakers, metallic foreign body and cochlear implants in situ, orthopedic hardware and those with movements artifacts were excluded.

Data and statistical analysis

The distribution of categorical variables like age categories, gender, levels, margins, shape, hilum, pericapsular spread, appearance on T1W, T2W, STIR image, necrosis, contrast enhancement, FNAC, diagnosis made on MRI, histopathology distribution, type of lymph nodes and diffusion restriction were studied. The association of ADC with type of lymph nodes were assessed using a chi-squared test. The mean difference in ADC between benign and malignant were compared using a student t-test. Receiver operating characteristic (ROC) curve of the ADC value used for differentiating benign from malignant lymph nodes. Accuracy of ADC Cut off value to differentiate benign from malignant lymph nodes were assessed a Kappa statistic. A p value of less than 0.05 was considered as statistically significant.

Results and Discussion

Patients were evaluated with Siemens MAGNETOM Avanto 1.5 T MRI machine. T1W, T2W, STIR and Diffusion weighted images were obtained. Enlarged cervical lymph nodes were studied and their levels were documented. Largest lymph nodes were identified in the individual and ROI was drawn over the solid component of the lymph node and ADC values were generated. Three ADC values were taken and average of these three values is considered for the study. Provisional diagnosis was given after studying the MRI features and correlated with histopathology findings in all cases. Total 71 cases included in our study in which 41 cases were of benign etiology and 30 were of malignant. (Table 1)

Out 41 benign cases of lymph nodes, 36 cases of reactive lymph nodes were correctly diagnosed, 4 cases of tuberculosis were correctly diagnosed and one case of necrotizing lymphadenitis was diagnosed as metastatic lymph node. Out of 30 malignant cases of lymph nodes, 27 cases were diagnosed correctly as metastatic lymph nodes, 2 lymphoma cases were diagnosed correctly as lymphoma and one lymphoma case was diagnosed as metastatic lymph node. (Table 2)

Metastatic cervical adenopathy [Figure 9 to 11]

Cervical nodal metastases have a major influence on the prognosis of patients with head and neck tumours. Imaging is used in the detection of nodal metastases at presentation and in the early detection of nodal tumour recurrence [8].

In a patient having a head and neck carcinoma, metastasis is suspected when a lymph node is greater than 1.5 cm in maximum diameter either in the jugulo-digastric region (level II) or in the submandibular triangles (level I) or when a node is greater than 1 cm in maximum diameter elsewhere in neck. These size criteria have been shown to be inaccurate in 20 to 28% of cases, either underestimating or overestimating the tumour [9].

Minimum axial diameter of a normal lymph node should not exceed 11 mm in the jugulo-digastric region and 10 mm elsewhere in the neck. Retropharyngeal nodes should not exceed 8 mm in maximum diameter or, 5 mm in minimum transverse diameter [10].

The ratio of the maximum longitudinal nodal length to the maximum axial nodal length (L/T) should be greater than 2 for normal hyperplastic nodes, while a value of less than 2 strongly suggests that the node contains metastatic carcinoma [10].

It has also been observed that a group of 3 or more lymph nodes with maximal diameter of 8 to 15 mm or minimum axial diameter of 9 to 10 mm in the jugulo-digastric region and 8 to 9 mm in the remaining neck are suggestive of metastatic lymphadenopathy, provided they are in the drainage area of the primary tumour [11].

Malignant and tuberculous nodes are usually round in shape. The short axis to long axis (S/L) ratio greater than or equal to 0.5 more favors for the malignant lymph node. The reactive and normal nodes are usually long or oval in shape. Nevertheless, it has been reported that normal submandibular and parotid nodes tend to be round in shape. Moreover, malignant nodes may be oval in shape when they are in early stage of involvement. Therefore, nodal shape should not be considered as the sole criterion in the diagnosis. However, eccentric cortical hypertrophy, which indicates focal intranodal tumour infiltration, is a useful sign to identify malignant nodes [12].

Central nodal necrosis is the most reliable radiological criterion for diagnosing nodal metastases. It typically manifests as an intra-nodal focal area of low attenuation with or without a surrounding rim of contrast enhancement on CT. Such an area may represent true necrosis, residual lymphoid elements, or tumour deposits. On T2-weighted MR images, a focal area of both high and intermediate

signal intensities is characteristically shown. Apart from being used as a radiological criterion for metastasis, central nodal necrosis may also be an important prognostic feature if the patient is treated with chemotherapy or radiotherapy. In cases of extensive necrosis, poor tumour oxygenation is probably the cause of resistance to chemotherapy and radiotherapy [13].

Majority of the tumour load enters a lymph node via the afferent lymphatics the tumour cells first start to proliferate within the node in the subcapsular region. So, occasionally on CT scans, low attenuation focal areas can be seen in these subcapsular nodal regions.

Histological presence of extra-nodal spread in 40% of lymph nodes less than 2 cm in diameter and 23% of lymph nodes 1 cm in greatest length has been reported. It is also known that when macroscopic transcapsular tumour spread is present, the patient has a nearly 10 times greater risk of recurrence [14].

The presence of extra-nodal tumour extension is identified on contrast enhanced CT and MRI as an enhancing, often thickened nodal rim usually with infiltration of adjacent fat planes. Kimura Y, Sumi M *et al.* suggested the possible criteria for extranodal spread on MR - nodal size (short-axis diameter), obliterated fat spaces between the metastatic node and adjacent tissues, such as the muscles and skin on T1-weighted images ("vanishing border" sign), the presence of high-intensity signals in the interstitial tissues around and extending from a metastatic node on fat-suppressed T2-weighted images ("flare" sign) and an irregular nodal margin on gadolinium-enhanced T1-weighted images ("shaggy margin") [13].

The extension of nodal tumour to adjacent internal carotid artery is a grave prognostic finding. This is identified by the degree of obliteration of the normal fat plane that surrounds the artery and the degree of the arterial circumference that is potentially involved by tumour. When more than 270 degree of the arterial circumference is surrounded by tumour, it is likely that the arterial wall has been invaded [15].

Of the primary head and neck tumours, the most common ones associated with nodal calcifications are metastatic papillary thyroid carcinomas. Nodal calcifications also occur with both Non-Hodgkin's and Hodgkin's lymphomas, particularly after irradiation and chemotherapy. Nodal calcification may also be seen in metastatic adenocarcinoma nodes, primary from breast, lung and colon tumours [16].

The degree of homogeneity of the signal intensity on contrast-enhanced T1-weighted images is an important criteria for differentiation between benign and malignant lymph nodes. A homogeneous enhancement was considered as normal. A heterogeneous enhancement was considered as indicative of metastatic lymph nodes. The third criterion was degree of homogeneity of the signal intensity on T2-weighted images. Homogeneous signal intensity was considered as normal. Heterogeneous signal intensity was considered as indicative of metastatic lymph nodes [14].

Reactive lymph nodes [figure 5]

Reactive lymph nodes are usually oval shaped, discrete, show homogeneous signal intensity with preserved fatty hilum without necrosis and without restricted diffusion on DWI **[16]**.

Tuberculous adenitis [Figure 6]

Cervical tuberculous adenitis is a manifestation of a systemic disease process [17].

It is most prevalent in the 20 to 30 years of age group, but can occur at any age. The most common site of involvement is the posterior triangle of neck followed by the supraclavicular fossa. The most common causative agents are Mycobacterium tuberculosis and atypical mycobacterium. The species of atypical mycobacterium that can cause lymphadenitis are-M. Kansasii, M. avium intracellulare and M. scrofulaceum. M scrofulaceum is the most common cause of cervical adenitis secondary to atypical mycobacterium. Three patterns have been described on MRI. These include discrete nodes, matted nodes, and confluent masses. Necrotic foci, when present, were more frequently peripheral rather than central, and this together with the soft tissue edema may be of value in differentiating tubercular nodes from metastatic nodes [18].

Lympho-proliferative disorders affecting neck [figure 12]

Lymphomas are subdivided into Hodgkin's Lymphoma and Non-Hodgkin's Lymphoma and are more specifically classified into subtypes of HL or NHL according to the WHO classification. CT is useful for staging and assessing bony involvement, whereas MR imaging is performed for soft tissue detail in extra-nodal disease, especially when there is intracranial or intra-spinal extension. Positron emission tomography has become an important part of staging and surveillance imaging and is particularly useful to distinguish post-treatment fibrosis from residual tumour. Lymphomas appear low in signal intensity on T1-weighted images and low to high in signal intensity on T2-weighted images, with variable, but usually low, enhancement following introduction of Gadolinium- DTPA contrast material [19].

Squamous cell carcinoma

Squamous cell carcinoma (SCC) accounts for the majority of the metastatic lymph nodes and is the most frequent malignancy of the head and neck region. It accounts for 5% of all malignant tumours worldwide **[20]**. It is most commonly seen in men older than 45years of age and is associated with tobacco and alcohol consumption. Patients with early-stage disease present with vague symptoms and minimal physical findings; the clinical presentation varies with the primary site involved. Head and neck SCCs are commonly located in the oral cavity, oropharynx, nasopharynx, hypopharynx and larynx [21]. Exact tumour staging is necessary for treatment planning, leading to reduced postoperative morbidity and tumour recurrence-associated mortality [22].

Submucosal extension cannot be sufficiently assessed by endoscopy and physical examination but can be evaluated with MRI or CT. CT and MRI are both useful for assessing deep tissue extensions of squamous cell carcinomas of the extra-cranial head and neck region that are stage T2 or greater. Once treatment is completed, a baseline scan 3 to 6 months following treatment is recommended in patients who are at risk for a later recurrence. For most primary tumour sites, MRI will give the most information concerning recurrent disease [23].

Sex

Out of the total 41 cases of benign lymph nodes 14(34.2%) were males and 27(65.9%) were females. (Table In all

benign cases we had 36 (50.7%) cases of reactive lymph nodes, 4 (5.6%) cases of tuberculosis and one(1.4%) case of necrotizing lymphadenitis.

Out of the total 30 cases of malignant lymph nodes 17(56.7%) were males and 13(43.3%) were female. In all malignant cases we had 13(18.3%) cases of carcinoma of tongue, 9 (12.7%) cases of carcinoma of buccal mucosa, 3 (4.2%) cases of lymphoma and one (1.4%) case of each adenocarcinoma of salivary gland, carcinoma of breast, carcinoma of esophagus, carcinoma of larynx and carcinoma of nasopharynx.

These findings correlate with the study conducted by Shah J. P *et al*, where they have observed that squamous cell carcinoma oral cavity is more common in males than females. It also states that chewing betel nut, with or without tobacco, a habit particularly prevalent in India, which is a strong risk factor for oral cancer **[24]**.

Age

The age of the patients included in our study varied from 3 to 70 years, with mean age of 42.8 years. Maximum numbers of patients were in the above 50 years age group (Table 3).

In our study maximum numbers of patients in the benign lymph nodes were in the age group of 21-30 years and patients with malignant lymph nodes were in the age group of above 50 years. The mean age for benign cases in our study was 35.2 years and for malignant cases was 50.9 years. (Table 4). This correlates with the study done Candela FC, Kothari *et al.* in 30 patients and they found that there is significant difference in the mean age group of benign and malignant patients which is due to the high incidence of malignancy in older age groups [25].

Region

In the study group the maximum number of lymph nodes were found at level II (95.8%) followed by level III (71.8%) then level IV (35.2%), level I (21.4%), level V (16.9%), supraclavicular level (5.6%) and least number of lymph nodes were seen at level VI (2.86). No lymph nodes seen at level VII in study group (Table 5). However only largest lymph node in each patient was studied for MRI and histopathology correlation. Out of 41 benign lymph nodes assessed 22 (53.7%) were present at the level II, 10 were seen in the level III, 2 (4.9%) were seen each at level Ib, IV, Va, and Vb and least 1 (2.4%) lymph node was at the level Ia. No benign lymph node was seen at level VI and VII in the study group. Out of 30 malignant lymph nodes assessed 17 (56.7%) were present at the level II, 8 (26.7%) were seen at the level III, 2 were seen each at the level Ib and V and least 1 (3.3%) lymph node was at the level IV. No malignant lymph node was seen at level VI, VII and supraclavicular in the study group. These findings correlate with study of Essing H *et al.* where they have seen in the most common metastatic lymph nodes in oral cavity cancers are seen at the level Ib and II [26].

Margins

Out of 41 cases of benign lymph nodes 37 (90.2%) lymph nodes showed regular margins and 4 (9.8%) showed irregular margins. (Table 6).

Out of these 4 benign lymph nodes of irregular margins 3 were of tuberculosis and one was the case of necrotizing lymphadenitis.

Out of 30 cases of malignant lymph nodes 25 (83%) lymph nodes showed irregular margins and 5 (16.7%) showed regular margins. These findings correlate with the study of R. B. J. de Bondt *et al.* in which he found that metastatic lymph nodes tend to have irregular, lobulated margins with perinodal fat stranding and benign lymph nodes tend to show regular smooth margins [27].

Shape

Out of 41 cases of benign lymph nodes 38 (92.7%) (%) lymph nodes were oval in shape and 3 (7.3%) were round in shape. (Table 6).

Out of 30 cases of malignant lymph nodes, 25(83.3%) cases of malignant lymph nodes were round in shape and 5 (16.7%) were oval in shape.

These findings correlate with the study of Ahuja AT *et al.* in which they found that metastatic and tuberculous lymph nodes tend to be round in shape with short axis to long axis (S/L) ratio greater than or equal to 0.5. The reactive benign lymph nodes which appears predominantly oval in shape. However malignant nodes may be oval in shape when they are in early stage of involvement [28].

Hilum

In our study group of 71 cases 36 (50.7%) lymph nodes showed preserved hilum and 35 (49.3%) lymph nodes showed altered hilum. (Table 6)

Out of 41 cases of benign lymph nodes 36 (87.8%) lymph nodes had preserved hilum and 5 (12.2%) had altered hilum. Out of these 5 benign lymph nodes, 4 were of tuberculosis and one was case of necrotizing lymphadenitis.

Out of 30 cases of malignant lymph nodes 28 (93.3%) lymph nodes had altered hilum and 2 (6.7%) had well preserved hilum.

These findings correlate with the study conducted by Kimura Y *et al.* where they found that loss of normal fatty hilum is one of the important features of the metastatic lymph nodes; however it is not always present in all malignant cases [13].

Peri-capsular Spread

In our study group of 71 cases 19 (26.8%) lymph nodes showed pericapsular spread and 52 (73.2%) lymph nodes did not show altered hilum. (Table 6)

Out of 41 cases of benign lymph nodes 38 (92.7%) lymph nodes did not show peri-capsular spread and 3 (7.3%) showed peri-capsular spread. These 3 benign lymph nodes were of tuberculosis.

Out of 30 cases of malignant lymph nodes 16 (53.32%) lymph nodes showed pericapsular spread and 14 (46.7%) lymph nodes did not show peri-capsular spread.

These findings correlate with the study conducted by Kimura Y *et al.* where they found that peri-capsular invasion is the one of determining factor of the malignant metastatic lymph nodes. In presence of pericapsular spread on contrast enhanced T1 weighted images lymph nodes show shaggy margins [13].

Intranodal necrosis

In our study group of 71 cases 31 (43.7%) lymph nodes showed presence of necrosis and 40 (56.3%) lymph nodes did not show necrosis. (Table 6)

Out of 41 cases of benign lymph nodes 37 (90.2%) lymph nodes did not show necrosis and 4 (9.8%) lymph nodes

showed presence of necrosis. Out of these 4 benign lymph nodes 3 were of tuberculosis and one was of necrotizing lymphadenitis.

Out of 30 cases of malignant lymph nodes 27 (90%) lymph nodes showed presence of necrosis and 3 (10%) lymph nodes did not show presence of necrosis.

These findings correlate with the study conducted by King AD *et al*, where they have found that necrosis is more common seen in the large metastatic lymph nodes and MRI is better than US for detection of necrosis. However several reports showed that these parameters are not enough to discriminate benign from malignant lesions [8].

Contrast enhancement

Out of 71 cases contrast study was performed in 45 cases, out of which 30 cases were of malignant lymph nodes and 15 cases were of benign lymph nodes. (Table 6)

Out of 30 cases of malignant lymph nodes 28 (93.3%) lymph nodes showed heterogeneous contrast enhancement and 2 (6.7%) lymph nodes showed homogeneous enhancement. These 2 cases of malignant lymph nodes showing homogeneous enhancement were of lymphomas.

Out of 15 cases of benign lymph nodes 10 (66.7%) lymph nodes showed homogeneous contrast enhancement, 3 (20%) lymph nodes showed heterogeneous enhancement and 2 (13.3%) lymph nodes showed peripheral contrast enhancement. These 10 cases of benign lymph nodes showing homogeneous contrast enhancement were of reactive lymph nodes, out of 3 cases showing heterogeneous enhancement one was case of necrotizing lymphadenitis and 2 cases were of tuberculosis and 2 cases showing peripheral contrast enhancement were of tuberculosis with large lymph nodal mass formation. These findings correlate with the study conducted by Cintra MB *et al.* where they found the heterogeneous contrast enhancement of lymph nodes is seen due to the presence of areas of necrosis and are more often seen in cases of malignant lesions [29].

Diffusion weighted imaging and ADC maps

Diffusion weighted image (DWI) is a non-invasive functional technique to study the molecular function and micro-structure of the tissue and lesion. It is use to study water motion in tissue and lesion. Every change in the water protons movements produces a variation in the signal of diffusion weighted images and as a result on ADC maps.

Diffusion weighted sequence was performed in all patients. ADC value was calculated in largest lymph nodes. Diffusion restriction was present in the 31 cases and was absent in the 41cases.

Out of 30 cases of malignant lymph nodes all 30 (100%) showed diffusion restriction and out of 41 cases of benign lymph node only one (2.4%) showed diffusion restriction (Table 7). The benign case which showed diffusion restriction was of necrotising lymphadenitis.

ADC values ranged from 0.4 to 1.3 $\times 10^{-3}$mm^2/s in our study group. The values of malignant lymph nodes ranged from 0.4 to 0.8 $\times 10^{-3}$mm/s and value of benign lymph nodes ranged from 0.8 to 1.3$\times 10^{-3}$ mm/s. (Table 8)

The mean ADC value calculated for benign lymph nodes was 1.1$\times 10^{-3}$mm^2/s (±0.9 SD) and the mean ADC value calculated for malignant lymph nodes was 0.7$\times 10^{-3}$ mm^2/s(±0.2 SD). (Table 9)

Receiver operating characteristic (ROC) curve of the ADC value was plot and ADC cut off value was suggested for differentiating benign from malignant lymph nodes. (Figure 4). The suggested ADC cut off value was 0.93$\times 10^{-3}$mm^2/s with the sensitivity of 97.6% and specificity of 100%. (Table 10)

These findings corroborate with the study conducted by Tamer Fali, where mean ADC value of benign lymph nodes was 1.56 ± 0.23$\times 10^{-3}$mm^2/s, for metastatic lymph node was 1.01 ± 0.23 $\times 10^{-3}$mm/s and for lymphoma was 0.71 ± 0.02 $\times 10^{-3}$mm^2/s. The cut off value of 1.15 $\times 10^{-3}$mm^2/s of ADC could differentiate benign from malignant lymph nodes. [30]

Our findings also correlate with study conducted by JichenWange *et al.*, Maysayuki Maeda *et al.*, Ann D King, R.J.de Bondt *et al.*, Holzopfel *et al.*, Vincent Vanecaveye, Anna Perrone *et al.*, Yaser G Abish *et al.*, Hazem M *et al.*, M.C lee *et al.*, J Si *et al.*, Ahmad Sabry Ragheb *et al*, Noha Abd ELShafy Saidetal, Jin Zhong *et al.*, Haitham A, Yeliz Pekcevik, Pratap Singh H Parihar *et al.*, C.H. Suh *et al.* All these studies demonstrate that diffusion weighted imaging with ADC threshold value can differentiate the benign and malignant lymph nodes [3, 4, 31-45].

However our findings did not correlate with study conducted by Hun Kung Lim *et al.* in which they concluded that mean ADC does not allow differentiating benign from metastatic cervical lymph nodes in patients with head and neck cancer and non-necrotic, small lymph nodes [46].

Limitations

Pericapsular spread, loss of fatty hilum, intranodal necrosis and heterogeneous contrast enhancement though commonly observed in malignant lymph nodes can be seen in benign etiology like tuberculosis, necrotizing lymphadenitis. As ADC value is influenced by factors like cellularity, vascularity and matrix of lymph node, there may be some overlap between benign and malignant cervical lymph nodes. Necrotic areas in metastatic lymph nodes show restricted diffusion with false high ADC values, hence ROI for calculating ADC values should be accurately placed in non-necrotic portion of metastatic lymph nodes.

Table 1: Histopathology Distribution

Histopathology	Number	Percentage
Benign Lymph nodes (n=41)		
Reactive lymph node	36	50.7
Tubercular lymph node	4	5.6
Necrotizing lymphadenitis	1	1.4
Malignant lymph node (n=30)		
Metastatic Lymph nodes		
Squamous cell carcinoma of tongue	13	18.3
Squamous cell carcinoma of buccal mucosa	9	12.7
Adeno carcinoma of salivary glands	1	1.4
Metastatic cervical lymph node from breast carcinoma	1	1.4
Squamous cell carcinoma of esophagus	1	1.4
Squamous cell carcinoma of larynx	1	1.4
Squamous cell carcinoma from nasopharynx	1	1.4
Lymphoma		
Non-Hodgkin's Lymphoma	3	4.2
Total	71	100

Table 2: Diagnosis made on MRI

MRI	Number	Percentage
Benign reactive	36	50.7
Metastatic	29	40.8
Tuberculosis	4	5.6
Lymphoma	2	2.8
Total	71	100

Table 3: Age Distribution

Age category in years	Number	Percentage
Less than 20	9	12.7
21-30	11	15.5
31-40	13	18.3
41-50	15	21.1
Above 50	23	32.4
Total	71	100

Table 4: Comparison of Mean age in years

Gender	Mean (SD)		T value	P value
	Benign (n=41)	Malignant (n=30)		
Age in years	35.2 (2.7)	50.9 (2.2)	4.5	<0.001

Table 5: Location of lymph nodes detected in study group

Level	Number	Percentage
I	15	21.4
II	68	95.8
III	51	71.8
IV	25	35.2
V	12	16.9
VI	2	2.8
VII	0	0
Supraclavicular	4	5.6

Table 6: Characteristics of benign and malignant cervical lymph nodes on various MRI sequences

Parameters	Benign	Malignant	P value
Margin			
Regular (n=42)	37 (90.2)	5 (16.7)	<0.001
Irregular (n=29)	4 (9.8)	25 (83.3)	
Shape of lymph node			
Round (n=28)	3 (7.3)	25 (83.3)	<0.001
Oval (n=43)	38 (92.7)	5 (16.7)	
Hilum			
Altered (n=33)	5 (12.2)	28 (93.3)	<0.001
Preserved (n=38)	36 (87.8)	2 (6.7)	
Pericapsular spread			
Present (n=19)	3 (7.3)	16 (53.3)	<0.001
Absent (n=52)	38 (92.7)	14 (46.7)	
T1WImages			
Homogeneous isointense (n= 40)	37 (90.2)	3 (10)	<0.001
Heterogeneous (n=31)	4 (9.8)	27 (90)	
T2W Images			
Homogeneous hyperintense (n=40)	37 (90.2)	3 (10)	<0.001
Heterogeneous hyperintense (n=31)	4 (9.8)	27 (90)	
STIR Image			
Homogeneous Hyperintense (n=40)	37 (90.2)	3 (10)	<0.001
Heterogeneous hyperintense(n=31)	4 (9.8)	27 (90)	
Intranodal necrosis			
Present (n=31)	4 (9.8)	27 (90)	<0.001
Absent (n=40)	37 (90.2)	3 (10)	
Contrast Enhancement			
Heterogeneous (n=31)	3 (20)	28 (93.3)	<0.001
Homogeneous (n=12)	10 (66.7)	2 (6.7)	
Peripheral (n=2)	2 (13.3)	0	

Table 7: Association of diffusion restriction with type of tumour

Diffusion restriction	Benign	Malignant	P value
Present (n=31)	1 (2.4)	30 (100)	<0.001
Absent (n=40)	40 (97.6)	0	
Total (n=71)	41 (100)	30 (100)	

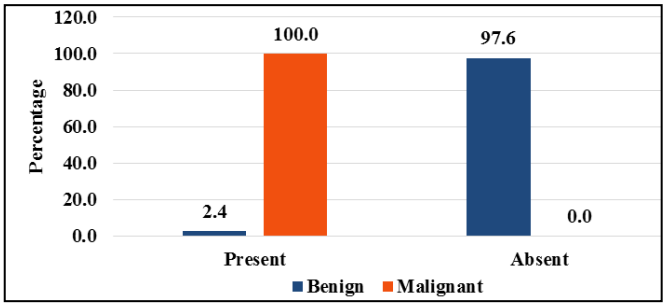

Fig 1: Association of Diffusion restriction according to type of tumour

Table 8: Association of ADC with type of lymph nodes

ADC values ($\times 10^{-3}$)	Malignant n (%)	Benign n (%)	P value
0.4-0.7	17 (56.7)	0	<0.001
0.7-1.0	13 (43.3)	1 (2.4)	
1.0-1.3	0	40 (97.6)	

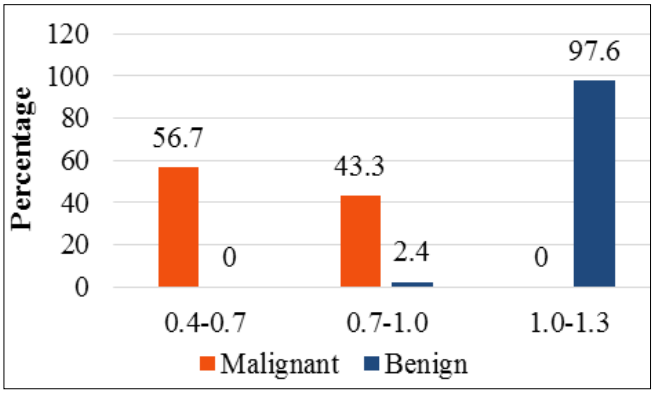

Fig 2: Association of ADC with type of lymph nodes

Table 9: Association of ADC with type of lymph nodes

Type of lymph nodes	N	Mean (SD) $\times 10^{-3}$ ADC	t	p-value
Benign	41	1.1(0.9)	18.9	<0.001
Malignant	30	0.7 (0.2)		

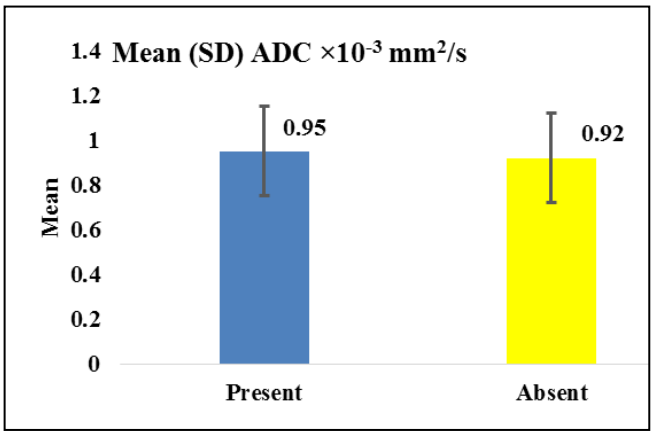

Fig 3: Association of ADC with type of lymph nodes

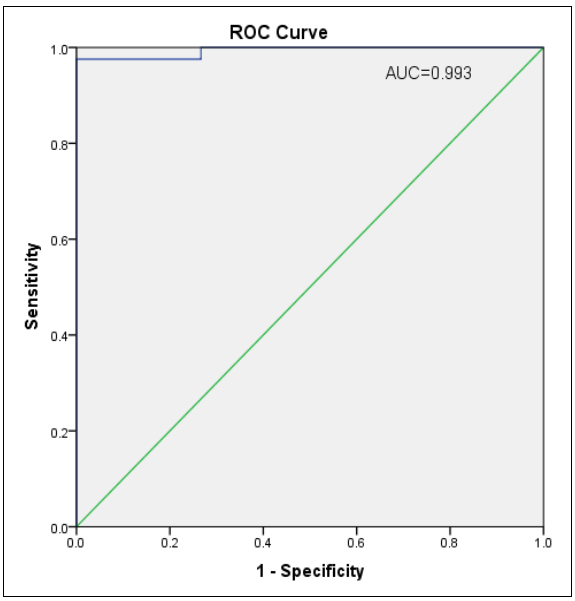

Fig 4: Receiver operating characteristic (ROC) curve of the ADC value used for differentiating benign from malignant lymph nodes.

Table 10: Suggested ADC Cut off value differentiating benign from malignant lymph nodes

ADC Cut off	Sensitivity	Specificity	PPV	NPV	AUC (95%C CI)
0.93 $\times 10^{-3}$	97.6%	100%	100%	96.7	0.993 (0.98-1)

Table 11: Comparison of ADC cut off and MRI findings

ADC cut off	MRI Findings		Kappa	P-Value
	Benign	Malignant		
$\geq 0.93 \times 10^{-3}$	40	1	0.97	<0.001
$<0.93 \times 10^{-3}$	0	30		

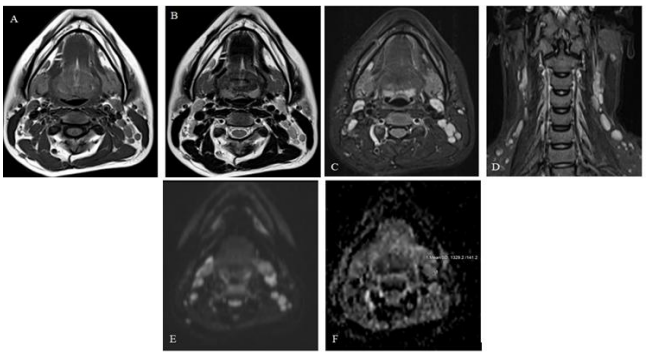

Fig 5: Benign reactive lymph nodes

MRI neck in 28 year female, with history of fever and swelling in the left side of neck 3 days, shows multiple well defined oval shaped lymph nodes at level II, III and IV bilaterally appearing homogenous iso-intense on T1WI (A), homogenous hyperintense on T2WI (B) and STIR (C,D). These lymph nodes on Diffusion weighted images do not show true restriction (E). The corresponding ADC value was found to be 1.329 × 10^{-3}mm^2/s (F).

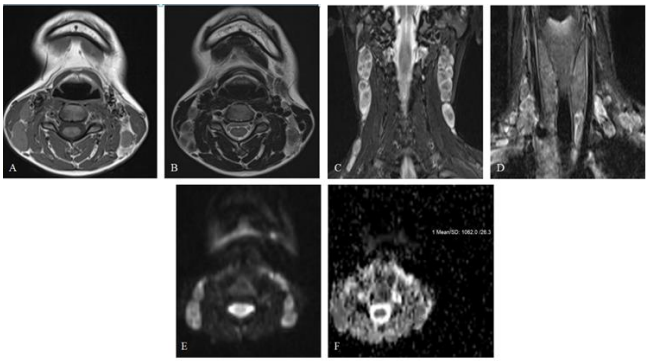

Fig 6: Tubercular lymph nodes

MRI neck in 21 year female, with history of fever, weight loss and swelling in neck on left side show multiple matted lymph nodes at level II, II, IV, V and in supraclavicular region bilaterally, appearing heterogeneously hypointense on T1WI (A), heterogeneously hyperintense on T2WI (B) and STIR (C, D).These lymph nodes do not show true diffusion restriction (E) with corresponding ADC values of 1.062 $\times 10^{-3}$mm^2/s(F).

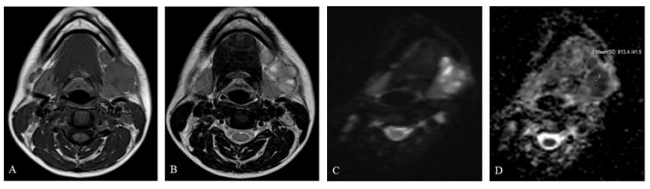

Fig 7: Necrotizing lymphadenitis

MRI neck in 17 years female with history of swelling in the left submandibular region and fever on and off show few enlarged necrotic lymph nodes at level IB on left side, appearing heterogeneously hypointense on T1WI (A) and T2WI (B). On diffusion weighted images (C) they show diffusion restriction with corresponding ADC values of 0.8134 $\times 10^{-3} mm^2/s$(D). MRI diagnosis was metastatic lymphadenopathy which turned out to be necrotizing lymphadenopathy on histopathology.

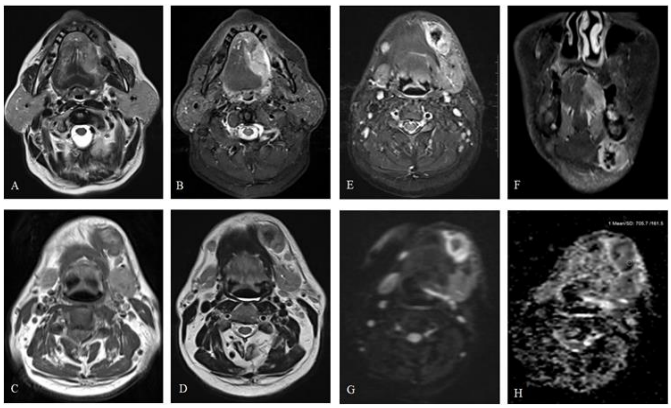

Fig 8: Carcinoma of tongue

MRI neck in 58- years male with history of ulcerative growth on tongue show ill -defined soft tissue intensity mass lesion in the anterior third of left half of tongue appearing heterogeneously hyperintense on T2WI (A) and STIR (B). Well defined enlarged lymph node with necrotic areas seen at level Ia and Ib appearing heterogeneous on T1WI (C) and heterogeneously hyperintense on T2WI (D). The lymph node appears heterogeneously hyperintense on STIR (E, F) and show diffusion restriction (G) with corresponding low ADC values of 0.7057 $\times 10^{-3} mm^2/s$ (H).

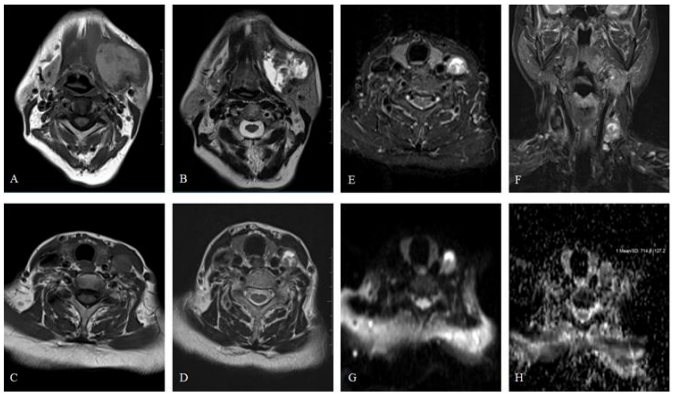

Fig 9: Carcinoma of the left submandibular salivary gland

MRI neck in 50- year female with history of swelling and pain over left mandibular region show an ill -defined soft tissue intensity lesion in the left submandibular salivary gland appearing heterogeneous on T1WI (A) and heterogeneously hyperintense on T2WI (B). A well-defined round shaped lymph node with areas of necrosis within seen at level III on left side appearing heterogeneously hypointense on T1WI (C) and heterogeneously hyperintense on T2WI (D). The lymph node appears heterogeneously hyperintense on STIR (E, F) and shows diffusion restriction (G) with corresponding low ADC value of 0.714 x 10^{-3} mm^2/sec (H).

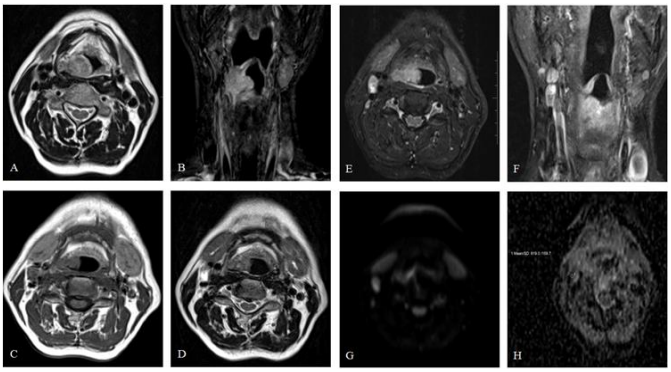

Fig 10: Carcinoma of right pyriform sinus

MRI neck in 47 -year male with history of pain in neck region shows well defined soft tissue intensity lesion involving the right aryepiglottic fold and right pyriform sinus appearing heterogeneously hyperintense on T2WI (A) and STIR (B). Well defined ovoid lymph node seen at the level II on right side appearing heterogeneously hypointense on T1WI (C) and heterogeneously hyperintense on T2WI (D). The lymph node appears heterogeneously hyperintense on STIR (E, F). It shows diffusion restriction (G) with corresponding low ADC value of 0.619 X $10^{-3} mm^2/sec$ (H).

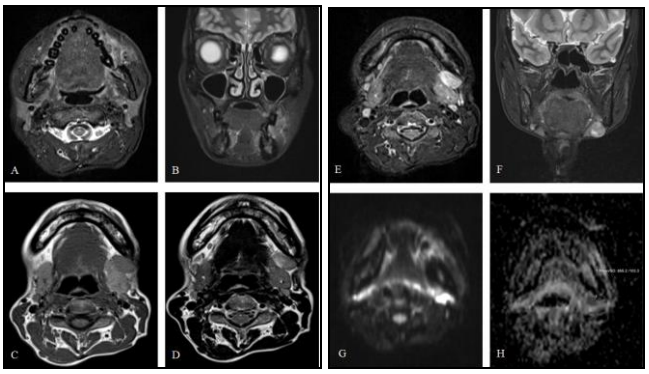

Fig 11: Case of carcinoma buccal mucosa

MRI neck in 50 -years old female with history of swelling in left submandibular region shows an ill-defined areas of altered singal intensity in left gingivobuccal sulcus extending to retro-molar trigone appearing heterogeneously hyperintense on STIR (A, B). Well defined enlarged lymph node seen at level Ib, appearing iso-intense on T1WI(C) and heterogeneously hyperintense on T2WI (D). This lymph node appears heterogeneously hyperintense on STIR (E, F) and show diffusion restriction (G) with low ADC value of 0.8552 $\times 10^{-3} mm^2/s$(H).

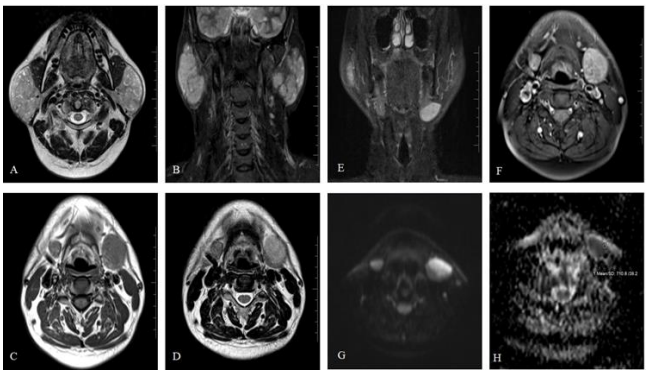

Fig 12: Lymphoma involving the bilateral Parotid glands

MRI neck in a 31- year old male with history of swelling in both parotid regions, shows bulky bilateral parotids appearing heterogeneously hyperintense on T2WI (A) and STIR (B). Well defined enlarged lymph node seen at level Ib appearing heterogeneously hypointense on T1WI (C) and heterogeneously hyperintense on T2WI (D). This lymph node appears hyperintense on STIR (E) and shows heterogeneous post-contrast enhancement (F). It shows diffusion restriction (G) with corresponding low ADC value of 0.7108 $\times 10^{-3} mm^2/s$ (H).

Conclusion

Magnetic resonance imaging (MRI) is an excellent modality for diagnosis of cervical lymph nodes and their exact location at various levels. MRI also helps to characterize the lymph nodes by their size, shape, margin, pericapsular spread, architecture, presence of necrosis and contrast enhancement pattern. Malignant lymph nodes tend to show diffusion restriction with corresponding low ADC values. The threshold ADC value of 0.93×10^{-3} mm^2/s could be used to differentiate between benign and malignant lymph nodes with 97.6% sensitivity and 100% specificity. Diffusion weighted imaging (DWI) is an important non-invasive diagnostic method for differentiation of benign and malignant cervical lymph nodes in case of head, neck cancers.

References

1. Kaji AV, Mohuchy T, Swartz JD. Imaging of cervical lymphadenopathy. Seminars in Ultrasound CT MR. 1999; 18(3):220-249.
2. Mack MG, Rieger J, Baghi M, Bisdas S, Vogl TJ. Cervical lymph nodes. European journal of radiology. 2008; 66(3):493-500.
3. Perrone A, Guerrisi P, Izzo L, D'Angeli I, Sassi S, Mele LL, Marini M *et al*. Diffusion-weighted MRI in cervical lymph nodes: differentiation between benign and malignant lesions. European journal of radiology. 2011; 77(2):281-6.
4. De Bondt RB, Hoeberigs MC, Nelemans PJ, Deserno WM, Peutz-Kootstra C, Kremer B *et al*. Diagnostic accuracy and additional value of diffusion-weighted imaging for discrimination of malignant cervical lymph nodes in head and neck squamous cell carcinoma. Neuroradiology. 2009; 51(3):183-92.
5. Sumi M, Sakihama N, Sumi T, Morikawa M, Uetani M, Kabasawa H *et al*. Discrimination of metastatic cervical lymph nodes with diffusion-weighted MR imaging in patients with head and neck cancer. American Journal of Neuroradiology. 2003; 24(8):1627-34.
6. Schafer J, Srinivasan A, Mukherji S. Diffusion magnetic resonance imaging in the head and neck. Magnetic Resonance Imaging Clinics. 2011; 19(1):55-67.
7. De Jong RJ, Rongen RJ, Verwoerd CD, van Overhagen H, Laméris JS, Knegt P. Ultrasound-guided fine-needle aspiration biopsy of neck nodes. Archives of Otolaryngology–Head & Neck Surgery. 1991; 117(4):402-4.
8. King AD, Tse GM, Ahuja AT, Yuen EH, Vlantis AC, To EW *et al*. Necrosis in metastatic neck nodes: diagnostic accuracy of CT, MR imaging, and US. Radiology. 2004; 230(3):720-6.
9. Som PM. Detection of metastasis in cervical lymph nodes: CT and MR criteria and differential diagnosis. AJR. American journal of roentgenology. 1992; 158(5):961-9.
10. Steinkamp HJ, Cornehl M, Hosten N, Pegios W, Vogl T, Felix R. Cervical lymphadenopathy: ratio of long-to short-axis diameter as a predictor of malignancy. The British journal of radiology. 1995; 68(807):266-70.
11. Van den Brekel MW, Castelijns JA, Snow GB. The size of lymph nodes in the neck on sonograms as a radiologic criteria for metastasis: how reliable is it? AJNR Am J Neuroradiol. 1998; 19(4):695-700.
12. Ng S, Ko S, Toh C, Chen Y. Imaging of neck metastases. Chang Gung medical journal. 2006; 29(2):119.
13. Kimura Y, Sumi M, Sakihama N, Tanaka F, Takahashi H, Nakamura T. MR imaging criteria for the prediction of extranodal spread of metastatic cancer in the neck. American Journal of Neuroradiology. 2008; 29(7):1355-9.
14. De Bondt RB, Nelemans PJ, Bakers F, Casselman JW, Peutz-Kootstra C, Kremer B *et al*. Morphological MRI criteria improve the detection of lymph node metastases in head and neck squamous cell carcinoma: multivariate logistic regression analysis of MRI features of cervical lymph nodes. European radiology. 2009; 19(3):626-33.
15. Yousem DM, Hatabu H, Hurst RW, Seigerman HM, Montone KT, Weinstein GS *et al*. Carotid artery invasion by head and neck masses: prediction with MR imaging. Radiology. 1995; 195(3):715-20.
16. Sakai O, Curtin HD, Romo LV, Som PM. Lymph node pathology: benign proliferative, lymphoma, and metastatic disease. Radiologic Clinics of North America. 2000; 38(5):979-98.
17. Vaid S, Lee YY, Rawat S, Luthra A, Shah D, Ahuja AT. Tuberculosis in the head and neck-a forgotten differential diagnosis. Clinical radiology. 2010; 65(1):73-81.
18. King AD, Ahuja AT, Metreweli C. MRI of tuberculous cervical lymphadenopathy. Journal of computer assisted tomography. 1999; 23(2):244-7.
19. Aiken AH, Glastonbury C. Imaging Hodgkin and non-Hodgkin lymphoma in the head and neck. Radiologic Clinics of North America. 2008; 46(2):363-78.
20. Dammann F, Horger M, Mueller-Berg M, Schlemmer H, Claussen C, Hoffman J *et al*. Rational diagnosis of squamous cell carcinoma of the head and neck region: comparative evaluation of CT, MRI, and 18FDG PET. American Journal of Roentgenology. 2005; 184(4):1326-31.
21. Marur S, Forastiere AA. Head and neck cancer: changing epidemiology, diagnosis, and treatment. In Mayo Clinic Proceedings Elsevier. 2008; 83(4):489-501.
22. Liu M, Weynand B, Delos M, Marbaix E. Prognostic factors in squamous cell carcinomas of the head and neck. Acta oto-rhino-laryngologica Belgica. 1999; 53(3):155-60.
23. Dillon WP, Harnsberger HR. The impact of radiologic imaging on staging of cancer of the head and neck. In Seminars in oncology. 1991; 18(2):64-79.
24. Shah JP, Candela FC, Poddar AK. The patterns of cervical lymph node metastases from squamous carcinoma of the oral cavity. Cancer. 1990; 66(1):109-13.

25. Candela FC, Kothari K, Shah JP. Patterns of cervical node metastases from squamous carcinoma of the oropharynx and Hypopharynx. Head & neck. 1990; 12(3):197-203.
26. Essig H, Warraich R, Zulfiqar G, Rana M, Eckardt AM, Gellrich NC *et al*. Assessment of cervical lymph node metastasis for therapeutic decision-making in squamous cell carcinoma of buccal mucosa: a prospective clinical analysis. World journal of surgical oncology. 2012; 10(1):253.
27. De Bondt RB, Nelemans PJ, Bakers F, Casselman JW, Peutz-Kootstra C, Kremer B *et al*. Morphological MRI criteria improve the detection of lymph node metastases in head and neck squamous cell carcinoma: multivariate logistic regression analysis of MRI features of cervical lymph nodes. European radiology. 2009; 19(3):626-33.
28. Ahuja AT, Ying M, Ho SY, Antonio G, Lee YP, King AD *et al*. Ultrasound of malignant cervical lymph nodes. Cancer Imaging. 2008; 8(1):48.
29. Cintra MB, Ricz H, Mafee MF, Santos AC. Magnetic resonance imaging: dynamic contrast enhancement and diffusion-weighted imaging to identify malignant cervical lymph nodes. Radiologia brasileira. 2018; 51(2):71-5.
30. Ali TF. Neck lymph nodes: characterization with diffusion-weighted MRI. The Egyptian Journal of Radiology and Nuclear Medicine. 2012; 43(2):173-81.
31. Wang J, Takashima S, Takayama F, Kawakami S, Saito A, Matsushita T *et al*. Head and neck lesions: characterization with diffusion-weighted echo-planar MR imaging. Radiology. 2001; 220(3):621-30.
32. Maeda M, Kato H, Sakuma H, Maier SE, Takeda K. Usefulness of the apparent diffusion coefficient in line scan diffusion-weighted imaging for distinguishing between squamous cell carcinomas and malignant lymphomas of the head and neck. American Journal of Neuroradiology. 2005; 26(5):1186-92.
33. King AD, Ahuja AT, Yeung DK, Fong DK, Lee YY, Lei KI *et al*. Malignant cervical lymphadenopathy: diagnostic accuracy of diffusion-weighted MR imaging. Radiology. 2007; 245(3):806-13.
34. Holzapfel K, Duetsch S, Fauser C, Eiber M, Rummeny EJ, Gaa J. Value of diffusion-weighted MR imaging in the differentiation between benign and malignant cervical lymph nodes. European journal of radiology. 2009; 72(3):381-7.
35. Vandecaveye V, De Keyzer F, Vander Poorten V, Dirix P, Verbeken E, Nuyts S *et al*. Head and neck squamous cell carcinoma: value of diffusion-weighted MR imaging for nodal staging. Radiology. 2009; 251(1):134-46.
36. Abish YG, Roshdy HM. Benign versus malignant cervical LNS: Differentiation by diffusion weighted MRI. AAMJ. 2011; 9(3):2.
37. El Shahat HM, Fahmy HS, Gouhar GK. Characterization of head and neck lesions with diffusion-weighted MR imaging and the apparent diffusion coefficient values. The Egyptian Journal of Radiology and Nuclear Medicine. 2013; 44(4):791-8.
38. Lee MC, Tsai HY, Chuang KS, Liu CK, Chen MK. Prediction of nodal metastasis in head and neck cancer using a 3T MRI ADC map. American Journal of Neuroradiology. 2013; 34(4):864-9.
39. Si J, Huang S, Shi H, Liu Z, Hu Q, Wang G *et al*. Usefulness of 3T diffusion-weighted MRI for discrimination of reactive and metastatic cervical lymph nodes in patients with oral squamous cell carcinoma: a pilot study. Dent maxillofacial Radiology. 2014; 43(3):20130202.
40. Ragheb AS, Rahman HM, Ismail AA, Nawar N. Can diffusion weighted image and apparent diffusion coefficient (ADC) differentiate benign from malignant cervical adenopathy?. The Egyptian Journal of Radiology and Nuclear Medicine. 2014; 45(2):377-86.
41. ElSaid NA, Nada OM, Habib YS, Semeisem AR, Khalifa NM. Diagnostic accuracy of diffusion weighted MRI in cervical lymphadenopathy cases correlated with pathology results. The Egyptian Journal of Radiology and Nuclear Medicine. 2014; 45(4):1115-25.
42. Barchetti F, Pranno N, Giraldi G, Sartori A, Gigli S, Barchetti G *et al*. The role of 3 Tesla diffusion-weighted imaging in the differential diagnosis of benign versus malignant cervical lymph nodes in patients with head and neck squamous cell carcinoma. BioMed research international, 2014.
43. Pekçevik Y, Çukurova İ, Arslan İB. Apparent diffusion coefficient for discriminating metastatic lymph nodes in patients with squamous cell carcinoma of the head and neck. Diagnostic and Interventional Radiology. 2015; 21(5):397.
44. Parihar P, Goel V. Differentiating benign and malignant metastatic cervical lymph nodes by diffusion weighted MRI sequence. International Journal of Anatomy Radiology and Surgery. 2015; 4(4):47-50.
45. Suh CH, Choi YJ, Baek JH, Lee JH. The diagnostic value of diffusion-weighted imaging in differentiating metastatic lymph nodes of head and neck squamous cell carcinoma: a systematic review and meta-analysis. American Journal of Neuroradiology. 2018; 39(10):1889-95.
46. Lim HK, Lee JH, Baek HJ, Kim N, Lee H, Park JW *et al*. Is diffusion-weighted MRI useful for differentiation of small non-necrotic cervical lymph nodes in patients with head and neck malignancies?. Korean journal of radiology. 2014; 15(6):810-6.